



Electrochemical determination of the organophosphate compound Fenamiphos and its main metabolite, Fenamiphos sulfoxide

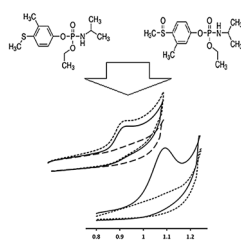
Bakhtiyar Qader^{1,2} · Mark G. Baron² · Issam Hussain³ · Robert P. Johnson² · Jose Gonzalez-Rodriguez²

Received: 14 September 2018 / Accepted: 14 November 2018 / Published online: 16 January 2019
© Springer-Verlag GmbH Austria, part of Springer Nature 2019

Abstract

A simple, rapid, and sensitive electrochemical method was developed for the determination of the organophosphate insecticide fenamiphos (FNP) and its main metabolite fenamiphos sulfoxide (FNX). The electrochemical behaviour was investigated by cyclic voltammetry and differential pulse voltammetry on a bare glassy carbon electrode. An oxidation peak was obtained for FNP and FNX at a bare glassy carbon electrode. The anodic peak showed irreversible behaviour and a mechanism of reaction at the electrode surface based on a mixed adsorption and diffusion controlled reaction is suggested. The obtained percentage of recovery showed good agreement compared to those reference values when GC–MS was used as a reference method.

Graphical abstract



Keywords Oxidation · Sensors · Electrochemistry · Pesticides · Cyclic voltammetry · Phosphorus compounds

Introduction

Fenamiphos (*O*-ethyl-*O*-(3-methyl-4-methylthiophenyl)-isopropylamido phosphate, FNP) is a colourless crystal or a tanned waxy solid organophosphorus pesticide (Fig. 1). It was first introduced in 1972 for the management of nematodes (roundworm) in plants. FNP is manufactured by the condensation of 4-(methylthio)-*m*-cresol with *O*-ethyl *N*-isopropyl phosphoramidochloride or reacting

4-methyl-*m*-cresol with ethylisopropylamido-phosphorochloride. The FNP and its oxidative products can easily penetrate underground waters due to its high solubility (0.4 g/dm³). Furthermore, in aquatic organisms approximately 1 mg/dm³ of FNP residues has been measured in areas of exposure remaining in the environment for long periods of time [1, 2]. Exposure to FNP may occur through many routes involving absorption from skin contact, ingestion of contaminated foods or drinking water, and aspiration of polluted material contaminated with FNP residues. An experimental study on rat and Guinea pig pointed out that FNP toxicity by inhalation is much higher than that through oral entry. FNP Lethal dose (LD50) in rats was found to be 2–19 mg/kg through oral route and 0.11–0.17 mg/dm³ via inhalation [3]. Stereoselective toxicity of FNP in aquatic organisms was also investigated and it was found that (–)-fenamiphos is 20 times less toxic than (+)-fenamiphos [4].

✉ Jose Gonzalez-Rodriguez
jgonzalezrodriguez@lincoln.ac.uk

¹ Sulaimani Medicolegal Institute, Qanat Street, Sulaimani, Kurdistan Regional Government, Iraq

² School of Chemistry, University of Lincoln, Lincoln, UK

³ School of Life Sciences, University of Lincoln, Lincoln, UK

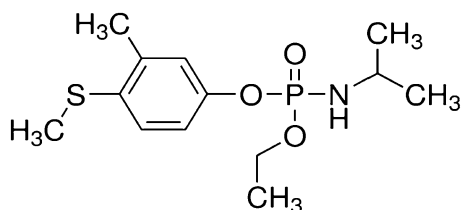


Fig. 1 Chemical structure of fenamiphos

Many analytical tools have been used for the determination of FNP and its metabolites in a wide range of samples, including nuclear magnetic resonance (NMR) [5], high-performance liquid chromatography (HPLC) [4], capillary electrophoresis (CE) [6], gas chromatography (GC) [7], and liquid chromatography–mass spectrometry (LC–MS) [8]. The *in vitro* metabolism for the biodegradation of FNP suggests a quick cleavage of P–O–C and P–N–C groups and the formation of CO₂ along with other main metabolites [9]. The main metabolites identified were fenamiphos sulfoxide (FNX), fenamiphos sulfone (FNO), and fenamiphos phenol (FP).

FNP is usually degraded after 63 days; however, in case of repeated application in the same soil, the degradation half-life is reduced to 14 days. The produced metabolites have the same toxic effects as the parent compound whilst their hydrolysed products did not show any toxicity [2]. Degradation of FNP in alkaline soil is more rapid than the degradation in acidic and neutral soils. Another possible route for the formation of FNX can be found through photolytic degradation of FNP in a period of over 3 h [2].

In the literature, there is little about the use of electrochemical analysis of FNP using different analytical approaches. In a first attempt, a study by Deng et al. [10] proposed that FNP was electrochemically inactive; hence, an EC biosensor based on *Escherichia coli* bacterial activity was introduced. Silk-derived carbon mat modified with Au@Pt nanoparticles (Au@Pt NPs) was utilized as a working electrode and provides a suitable microenvironment media for the bacteria. Square wave voltammetry was used for the measurement of EC signal using the inhibitory effect of FNP on bacterial activity. The suggested method was capable of detecting FNP from 0.5 to 36.6 mg/dm³ with a good linearity and LOD of 0.09 mg/dm³ (0.3 μM) [10]. Electrochemical quantification of FNP and another pesticide, carbendazim, in natural water samples was achieved on a diamond electrode. In this work, the electrochemical activity of FNP using cyclic voltammetry (CV) and SWV techniques was proved for the first time. In CV experiments, FNP showed an irreversible oxidation peak at potential of 1.2 V vs. Ag/AgCl in 0.1 M Na₂HPO₄ solution. A linear calibration curve was performed using SWV measurements in a range of 0.5–25 μM while the LOD was established at 0.1 μM. The suggested

method proved not directly feasible for simultaneous determination of FNP and carbendazim [11]. Consequently, an experimental design based on a chemometric approach was conducted for the simultaneous measurement of carbendazim and FNP using boron-doped diamond electrodes. The study confirmed the irreversible oxidation of FNP with their best peak intensity at pH 2. The SWV technique was utilized for producing a regression curve in a concentration range of 4.95–36.7 μM for FNP with an LOD of 4.1 μM. Another voltammetric method was applied for analysis of FNP in lemon juice samples with a recovery rate of 92.5% [12]. Both previous methods did not point out a mechanistic behaviour of FNP. No other electrochemical methods reported the analysis of its major metabolite, FNX.

The aim of this paper is to fill the gap on the electrochemical analysis of organophosphates and their metabolites with environmental and forensic interest as these can be used as chemical warfare agents or pollutants of the environment. The previous work from the authors on electrochemical determination of 2-isopropoxyphenol [13] and disulfoton [14] is evidence that the design of sensors for the determination of these compounds in biological or environmental samples is highly important. Electrochemical methods based on carbon solid electrodes can play an important role as field screening methods for *in situ* applications.

Results and discussion

CV was used for the voltammetric study of FNP and FNX after a full reduction and oxidation scan performed by CV at bare glassy carbon (GC) electrode surface. A well-defined single oxidation peak was noted for FNP at potential of 1.087 V and 0.887 V for FNX (vs. Ag/AgCl) in BR buffer solution. Fenamiphos sulfone (FNO) is also another metabolite of FNP and shown for comparison in Fig. 2. The nature of the reaction is in both cases irreversible due to the absence of reduction peak upon reverse scan potential (Fig. 2).

To show the potential influence of the different buffers and supporting electrolyte solutions on the FNP peak intensity, various buffers and supporting electrolytes with the same concentration (0.1 M) were tested. These were: sodium chloride (NaCl), sodium perchlorate (NaClO₄), lithium perchlorate (LiClO₄), sulfuric acid (H₂SO₄), Britton–Robinson (BR) buffer at pH 3, potassium nitrate (KNO₃), and phosphate-buffered saline at pH 3 (PBS). The best response for the oxidation peak of FNP was achieved using the BR buffer solution as shown in Fig. 3.

The oxidation peak of FNP and FNX was investigated by differential pulse voltammetry (DPV) in a pH range 2–9 in a BR buffer. The anodic peaks of the FNP showed no

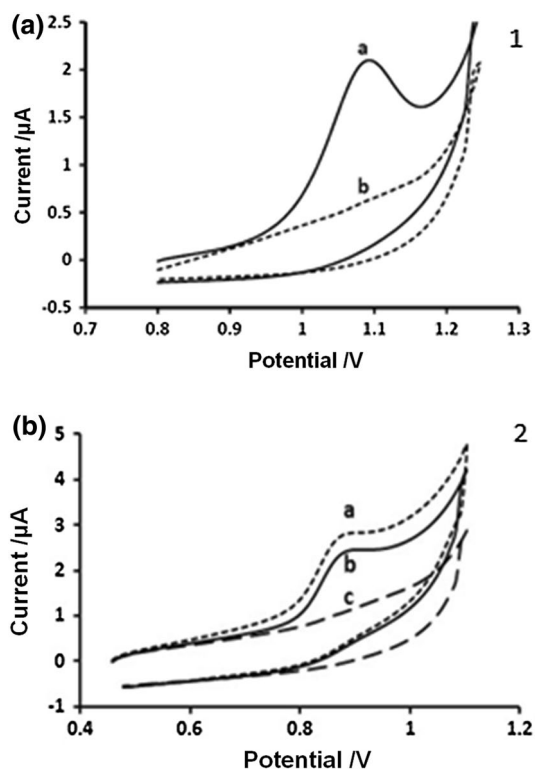


Fig. 2 Cyclic voltammogram of 1(a) 45 μM fenamiphos; 1(b) blank and 2(a) 50 μM FNO; 2(b) 50 μM FNX and 2(c) blank in 0.1 M Britton–Robinson buffer solution (pH 3 and pH 6, respectively) on bare glassy carbon electrode at potential scan rate 100 mV

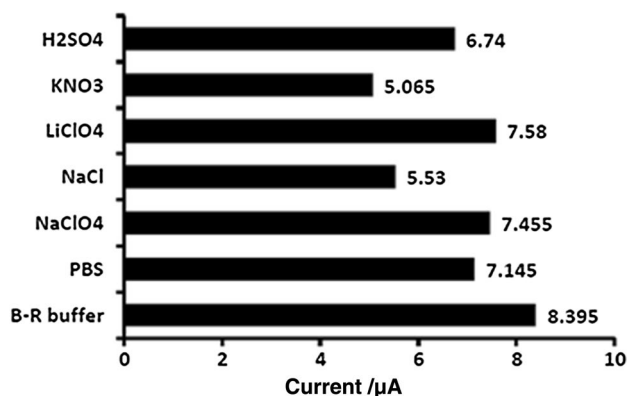


Fig. 3 Influence of various buffers and supporting electrolytes on oxidation peak of 0.1 mM FNP on GC electrode

obvious change of peak potential with changing the pH of the solution (Fig. 4).

A plot of peak potential vs. pH later confirmed that the peak potential does not effectively change with increasing pH suggesting that there is no involvement of protons in the overall electrode reactions. Furthermore, the peak current intensity was found to increase with decreasing pH values and the optimum current response was found at pH 3

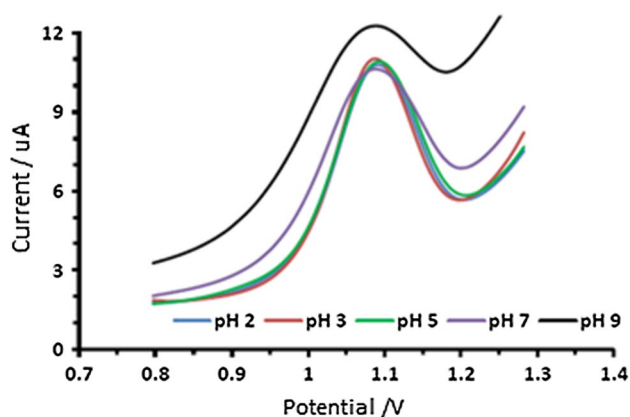


Fig. 4 Differential pulse voltammogram of 0.1 mM FNP at pH value range 2–9 in 0.1 M BR buffer at bare GC electrode

(Fig. 5). In the case of FNX, the influence of pH on oxidation peak of FNX was investigated in 0.1 M BR buffer in the pH range 3–9. The peak potential shifted toward positive direction with increasing pH values following the equation: $E_p = -0.0599 \text{ pH} + 1.246$ ($r^2 = 0.9745$) (Fig. 6).

The effect of scan rates ν on the oxidation of FNP was also studied within the range 10–1000 mV/s. The peak potential was shifted positively when the scan rate was increased confirming the irreversibility of the oxidation reactions. A linear response was observed with the square root of scan rates and their corresponding current response suggesting that the reaction process is controlled by diffusion. In addition, a value of logarithm of peak intensity ($\log I_p$) was in a linear relationship with a value of logarithm of scan rate ($\log \nu$). The linearity is expressed in equation $\log I_p = 0.9256 \log \nu + 1.9497$ ($r^2 = 0.999$) with a slope value of 0.92 close enough to the theoretical value of 1.0 (adsorption control) confirming that the reaction process is adsorption–diffusion controlled. In the case of FNX, the $\log I_p = 0.779 \log \nu + 1.2488$ ($r^2 = 0.9987$) was obtained. The slope of the equation is 0.77 which is a value in between theoretical value of 0.5 (diffusion control) and value of 1 (adsorption control). This observation is suggesting that the reaction at the electrode surface is a complex mechanism.

To assess the number of electrons transferred in the oxidation reaction of FNP, a plot of peak potential (E_p) versus logarithm scan rate ($\log \nu$) was done in sweep rate range 10–1000 mV/s. The equation obtained was $E_p = 0.0616 \log \nu + 1.0998$ ($r^2 = 0.9806$). Using the Laviron procedure for irreversible species, the α_n value calculated is equal to 0.95. Also, α can be calculated as $\alpha = 47.7/E_p - E_{p/2}$ mV where $E_{p/2}$ is the potential where the current is at half the peak value. For this system, a value of α was calculated to be 0.79. Hence, the number of electrons (n) shared in the oxidation reaction of IPP is equal to $1.2 \approx 1$. In the case of FNX, $\log E_p = 0.0619 \log \nu + 0.9365$, $r^2 = 0.9369$ was obtained and α_n

Fig. 5 **a** Influence of pH on potential peak; **b** influence of pH on current response; of 0.1 mM FNP at pH value range 2–9 in 0.1 M B–R buffer on bare GC electrode

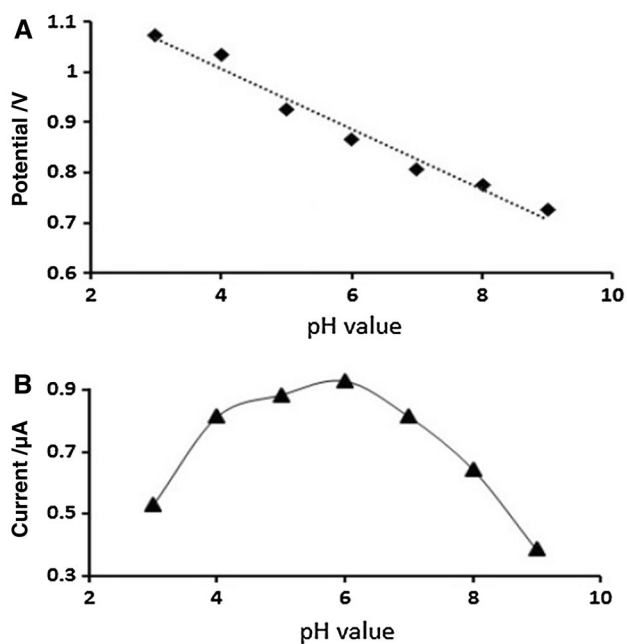
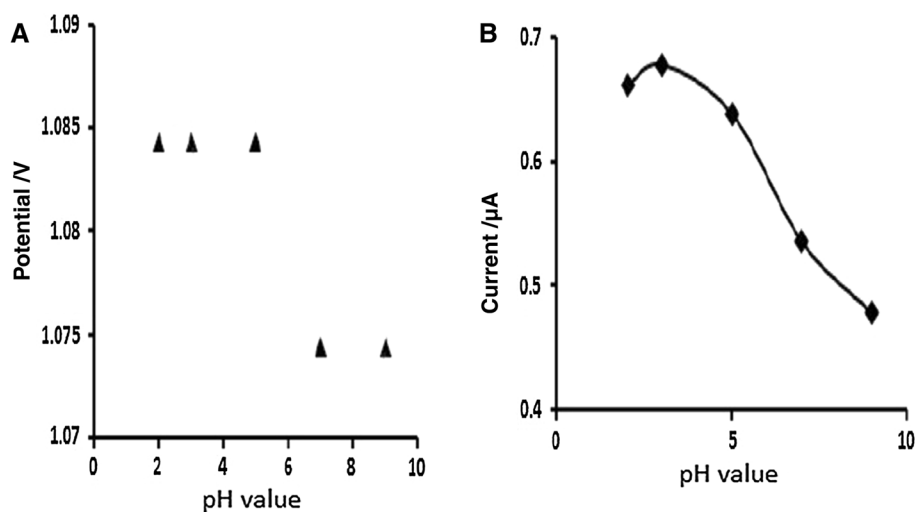


Fig. 6 **a** Influence of pH on potential peak; **b** influence of pH on current response; of 50 µM FNX in 0.1 M B–R buffer on bare GC electrode

value calculated is equal to 0.93. The number of electrons calculated using the same scheme than for FNP was $1.15 \approx 1$ for FNX.

Roberts and Hutson [9] proposed an *in vitro* biological metabolic pathway for FNP and FNX. The results obtained in our study also support the mono-electronic oxidation mechanism.

The calibration curves showed good linear responses within the concentration range 8–75 µM and from 5 to 75 µM with coefficient of determination $r^2 = 0.9981$ and 0.9976 using CV and DPV, respectively, for FNP. In the

case of FNX, the calibration curves also showed good linear responses within the concentration range from 8 to 70 µM and from 7 to 70 µM with coefficient of determination $r^2 = 0.9991$ and 0.9987 using CV and DPV, respectively.

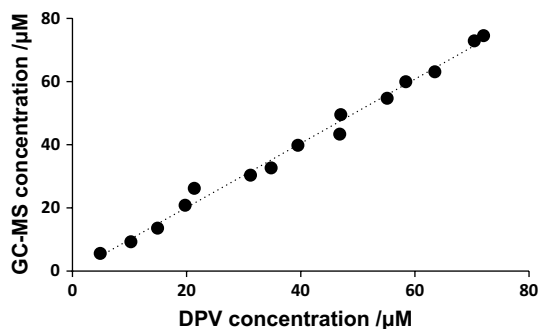
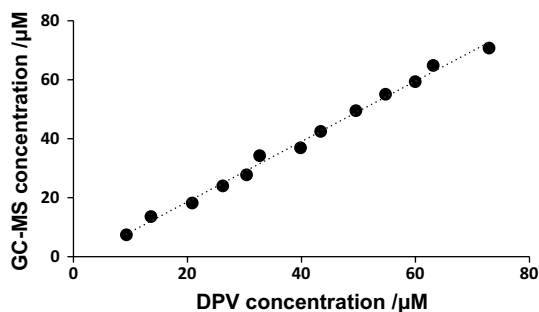
A summary of the analytical characteristics obtained for both FNP and FNX can be found in Table 1. Intra-day precision was calculated with five measurements from the same concentration in the same day, whereas interday precision was calculated using measurements obtained in five consecutive days. All values were calculated using a calibration curve obtained in the day.

To validate the developed method, the same concentrations of FNP and FNX were also injected in a GC–MS used as a reference method to compare with recovery results from electrochemical system. In FNP, the results showed a good linear correlation for CV ($y/\mu\text{M} = 0.9952 \pm 0.0201$ $x/\mu\text{M} + 0.6502 \pm 0.9058/\mu\text{M}$, $r^2 = 0.9947$) and DPV ($y = 1.016 \pm 0.0266$ $x/\mu\text{M} - 0.1895 \pm 1.1900/\mu\text{M}$, $r^2 = 0.9912$) (Fig. 7). In FNX, the results also showed a good linear correlation for CV ($y = 1.0111 \pm 0.0402$ $x/\mu\text{M} - 0.2511 \pm 1.7758/\mu\text{M}$, $r^2 = 0.9844$) and DPV ($y = 1.022 \pm 0.0234$ $x/\mu\text{M} - 1.847 \pm 1.0323/\mu\text{M}$, $r^2 = 0.9942$) (Fig. 8).

To evaluate the validity of the proposed electrochemical method for the determination of FNP and its major metabolite (FNX) in real samples, human plasma and urine samples were spiked with known amount of FNP or FNX. 1 cm³ of synthetic human plasma was added to 29 cm³ of BR buffer solution. Accordingly, 2 cm³ of fresh urine sample was taken and diluted to 30 cm³ with the BR buffer solution and then directly analysed. Two different concentrations of FNP or FNX were added into the plasma and urine sample solutions before measuring with CV or DPV using the bare GC electrode. The calibration graph for each of the methods was used to calculate the recovered concentration of the spiked samples. Table 2 includes the results obtained from CV and

Table 1 Analytical characteristics for both FNP and FNX using CV and DPV

	Analytical technique	Conc/ μM	Mean ^a / μM	Recovery ^a /%	RSD ^a /%	RSD ^b /%	LoD/ μM	LoQ/ μM
FNP	CV	8	9.67 \pm 0.13	120.87	1.34	10.44	0.94	3.14
		45	46.05 \pm 1.16	102.34	2.53	4.84		
	DPV	5	4.85 \pm 0.14	97.09	3.03	9.15	0.68	2.29
		45	46.83 \pm 1.07	104.06	2.28	4.63		
FNX	CV	8	8.14 \pm 0.96	101.83	11.79	12.99	1.13	3.44
		40	42.13 \pm 1.22	105.33	2.90	3.27		
	DPV	7	7.42 \pm 0.45	106.01	6.06	8.87	0.67	2.03
		40	36.89 \pm 2.83	92.23	7.00	7.67		

^aIntraday ($n=5$)^bInterday ($n=5$)**Fig. 7** Comparison of concentration values (8, 10, 15, 20, 25, 30, 35, 40, 45, 50, 55, 60, 65, 70, and 75 μM) FNP obtained in the experimental set with GC/MS and DPV ($n=3$ for each concentration)**Fig. 8** Comparison of concentration values (8, 15, 20, 25, 30, 35, 40, 45, 50, 55, 60, 65, and 70 μM) FNX obtain in the experimental set with GC/MS and DPV ($n=3$ for each concentration)

DPV analysis at bare GC electrode for recovered concentrations of FNP in urine and plasma samples. The recovery rate was noted in a range of 80.81–96.37% and the %RSD value is less than 10.97%. Table 3 includes the results obtained by CV and DPV analysis at the bare GC electrode for the different concentrations of FNX in urine and plasma samples. The recovery rate was noted in a range of 70.5–92.94% and the %RSD value is less than 19.28%. Thus, the results showed

that the matrix did not significantly influence the recovered concentration. Moreover, urine matrix has slightly less effect on recovered concentration than plasma.

Conclusion

Both FNP and FNX showed electroactivity on GC carbon electrode using CV and DPV. An oxidation peak was obtained for both analytes at the bare GC electrode using a BR buffer solution with optimum peak intensity at pH 3 in the case of FNP and pH 6 for FNX. The anodic peak showed irreversible behaviour and the irreversibility of the system was confirmed using the scan rates. It was found that increasing concentrations of both FNP and FNX in the buffer solution proportionally increased the signal. The anodic peak showed a reliable intraday and interday precision. The analysed concentrations showed good agreement compared to those reference values when GC–MS was used as a reference method. FNP and FNX were recovered in spiked plasma and urine samples with acceptable results using developed methods.

Experimental

Fenamiphos (FNP) and fenamiphos sulfoxide (FNX) were obtained from Sigma (Sigma-Aldrich, UK). Sodium perchlorate and lithium perchlorate were ordered from Fisher Scientific (Fisher Scientific, UK). Potassium chloride, Tris buffer, and sodium acetate buffer were obtained from Sigma (Sigma-Aldrich, UK). Potassium monophosphate and potassium dibasic phosphate were bought from Fisher Scientific (Fisher Scientific, UK). Phosphoric acid, hydrochloric acid, and potassium hydroxide were all purchased from Fisher Scientific (Fisher Scientific, UK); sodium chloride was bought from Sigma (Sigma-Aldrich, UK). Britton–Robinson buffer solution was made of phosphoric acid, glacial acetic

Table 2 Recoveries from spiked urine and plasma samples for two known concentrations of FNP using CV and DPV measurements at bare glassy carbon electrode

Interference media	Analytical technique	Concentration spiked/ μM	Mean/ μM	Recovery/%	RSD/%
Plasma, $N=3$	CV	15	13.44	89.64	8.89
		25	22.83	91.32	10.81
	DPV	15	12.8	85.39	2.52
		25	22.77	91.10	6.20
Urine, $N=3$	CV	15	13.29	88.64	10.97
		25	23.50	94.03	3.16
	DPV	15	12.12	80.81	1.76
		25	24.09	96.37	8.57

Table 3 Recoveries from spiked urine and plasma samples for known concentrations of FNX using CV and DPV measurements at bare glassy carbon electrode

Interference media	Analytical technique	Concentration spiked/ μM	Mean/ μM	Recovery/%	RSD/%
Plasma, $N=3$	CV	15	10.57	70.51	19.28
		25	22.27	89.10	11.32
	DPV	15	12.81	85.44	14.31
		25	22.19	88.79	2.20
Urine, $N=3$	CV	15	12.66	84.40	4.70
		25	23.23	92.94	5.40
	DPV	15	12.31	82.11	8.65
		25	22.99	91.98	3.24

acid and sodium chloride; the pH value was adjusted with sodium hydroxide and hydrochloric acid. Potassium ferric cyanide was purchased from Sigma-Aldrich (Sigma-Aldrich, USA) and used to test the polished glassy carbon electrode. Fumed silica (particle size $0.007 \mu\text{M}$) and aluminium oxide (particle size $0.05 \mu\text{M}$) were used for polishing the glassy carbon electrode and both were bought from Sigma-Aldrich (Sigma-Aldrich, UK). Acetonitrile (HPLC grade) from Fisher (Fisher Scientific, UK) was used in the sonication of the GC electrode. Water was purified using an ELGA purification system to a specific resistance $18 \text{ M}\Omega$ and used to prepare all solutions. Artificial human plasma was purchased from Sigma (Sigma-Aldrich, UK). Urine aliquot was freshly taken from a volunteer.

Voltammetric experiments were performed using a Metrohm 757 VA Computrace (Metrohm Ltd., UK); data processing software is Metrohm version 1.0 Ct757 software (Metrohm Ltd., UK), running on a personal computer (Compaq® DeskPro, Windows® 95). A conventional three-electrode system was used for all the experiments, which consisted of a glassy carbon (GC) working electrode, an Ag/AgCl reference electrode and platinum as an auxiliary electrode. All electrodes were purchased from Metrohm (Metrohm Ltd., UK). A digital pH meter (Hanna instrument microprocessor pH 210 m) was used when preparing buffer solutions. An ultrasound bath (Kerry, UK) was used for electrode sonication. GC-MS components were from Perkin

Elmer (USA). GC model Clarus 500 equipped with an auto sampler and MS model Clarus 500 operated with Perkin Elmer TurboMass (2008) software. Standards and samples were run on an SUPELCO analytical SLB-5 m fused silica capillary column ($30 \text{ m} \times 0.25 \text{ mm} \times 0.25 \mu\text{M}$).

FNX and FNP solutions were prepared as 30 mmol and 15 mmol standard stock solutions in acetonitrile and stored at $-8 \text{ }^\circ\text{C}$ until use. All other working solutions were freshly prepared from the standard stock solution. Britton-Robinson buffer (BRB) is an aqueous universal buffer that was used for the pH study in the range of 1.6–12. A 0.5 mol/dm^3 of BRB was prepared by combining 33.8 cm^3 of concentrated phosphoric acid, 28.6 cm^3 of concentrated acetic acid and 29.22 g of sodium chloride. The pH value was adjusted with sodium hydroxide and hydrochloric acid and then made up to 1 dm^3 with distilled water.

Prior to running all experiments, the GC electrode was polished to a mirror-like surface successively with activated aluminium oxide and $0.007 \mu\text{M}$ silica slurry. The electrode was thoroughly washed with water and then treated with acetonitrile in an ultrasonic bath for about 5 min. Electrochemical experiments were carried out in a 50 cm^3 voltammetric cell at room temperature and the electrochemical measurements were performed after initial purging of the mixture under nitrogen gas for 300 s. The cleaned bare GC electrode was tested by CV in $0.01 \text{ mol/dm}^3 \text{ K}_3[\text{Fe}(\text{CN})_6]$ solution with scan rate of 0.1 V/s within the potential range of -1.0

to + 1.0 V (vs. Ag/AgCl) until a pair of well-defined redox peaks was obtained. Cyclic voltammetry (CV) measurements were achieved in the potential range from 0.6 to 1.3 V with a scan rate of 100 mV/s, and equilibrium time of 10 s. Differential pulse voltammetry (DPV) measurements were performed in the potential range from 0.6 to 1.3 V with voltage step, 0.009918 V; pulse amplitude, 50 mV; pulse time, 0.04 s; voltage step time, 0.4 s, and sweep rate, 0.0248 V/s.

For GC–MS analyses, the oven temperature started at 100 °C, held for 1 min, and was then increased at 25 °C/min to 200 °C, held for a further 2 min, and finally ramped at 10 °C/min was to reach a final temperature of 310 °C which is held for 2 min. The carrier gas was helium at 1 cm³/min and the injection volume was 2 mm³. The transfer line temperature was held at 300 °C. Positive ionization was performed using an electron impact (EI+) source at 200 °C with electron energy of 70 eV and the multiplier was set to 350 V. The peaks were observed in total ion count (TIC) mode after 2 min solvent delay giving a total run time of 20 min.

Acknowledgements The authors gratefully acknowledge the financial support of this work by the Higher Committee for Educational Development (HCED number D-11-3277), Iraq.

References

1. Caceres T, Megharaj M, Naidu R (2009) *Sci Total Environ* 398:53
2. Caceres T, Megharaj M, Malik S, Beer M, Naidu R (2009) *Biore-sour Tech* 100:732
3. Abu Ghalwa NM, Farhat NB (2016) *J Environ Anal Tox* 6:1
4. De Albuquerque NC, De Matos JV, De Oliveira AR (2016) *J Chromatogr A* 1467:326
5. Molaabasi F, Talebpour Z (2011) *J Agric Food Chem* 59:803
6. Lecoeur-Lorin M, Delepee R, Morin P (2009) *Electrophoresis* 30:2931
7. Hernandez-Borges J, Juan Cabrera JC, Rodriguez-Delgado MA, Hernandez-Suarez EM, Galan Sauco V (2009) *Food Chem* 113:313
8. Asensio-Ramos M, D'orazio G, Hernandez-Borges J, Rocco A, Fanali S (2011) *Anal Bioanal Chem* 400:1113
9. Roberts T, Hutson D (1999) *Metabolic pathways of agrochemicals: part two—insecticides and fungicides*. RSC, UK
10. Deng L, Guo S, Zhou M, Liu L, Liu C, Dong S (2010) *Biosens Bioelectron* 25:2189
11. Franca RF, De Oliveira HPM, Pedrosa VA, Codognoto L (2012) *Diam Relat Mater* 27–28:54
12. Lima T, Silva HTD, Labuto G, Simoes FR, Codognoto L (2015) *Electroanalysis* 28:817
13. Qader B, Baron MG, Hussain I, Gonzalez-Rodriguez J (2018) *J Electroanal Chem* 821:16
14. Qader B, Baron MG, Hussain I, Sevilla JM, Johnson RP, Gonzalez-Rodriguez J (2018) *Electrochim Acta* 295:333